Oxygen Speciation in Nanophase MgO from Solid-State ^{17}O NMR

Alan V. Chadwick, Iain J. F. Poplett, David T. S. Maitland, and Mark E. Smith*

Centre for Materials Research, School of Physical Sciences, University of Kent, Canterbury, Kent, U.K. CT2 7NR

Received September 17, 1997. Revised Manuscript Received November 6, 1997

Nanocrystalline MgO has been sol−gel manufactured to give a range of crystallite sizes from 1.8 to 35 nm as determined by powder X-ray diffraction. A multinuclear magnetic resonance approach using ^{13}C, ^{17}O, and ^{25}Mg provides information on the atomic scale structure. It is found that despite extensive hydrolysis that $-CH_3$ fragments persist until extensive calcination has been performed. In ^{17}O magic angle spinning NMR spectra three signals are detected that are assigned to MgO-like, a surface species, and a unit also like MgO but with carbon as the third nearest neighbor, demonstrating the high sensitivity of the ^{17}O chemical shift to local structure and its ability to detect medium-range order.

Introduction

There is a growing interest in nanocrystalline materials since their properties can be markedly different from the parent bulk solids.[1,2] Such interest in nanocrystalline oxides results from the possibilities of producing superhard and superplastic ceramics and for catalysts where the increased surface area to volume ratio available for nanocrystalline forms will greatly enhance activity. However, recent work on simple binary oxides[3−5] suggests other factors i.e., surface morphology and surface chemistry are advantageously different for nanocrystals. In addition, nanocrystalline materials will dissolve higher concentrations of impurities than their bulk counterparts, and this offers further scope for tailoring new catalytic materials. A thorough understanding of the chemistry of these new materials depends on detailed structural characterization and the link to preparation conditions. In this paper new structural information is reported for nanocrystalline magnesium oxide using solid-state ^{17}O NMR.

From both the technological and academic viewpoints MgO is one of the most important ionic solids. MgO is widely used as a catalyst[6,7] (particularly for oxidative coupling of methane[8]) and as an insulating ceramic[9] and is finding applications in the semiconducting industry as a thin-film intermediate substrate for other metal oxide layers.[10] Single crystals are readily available, and there have been extensive experimental studies of the defect[11] and surface chemistry.[12] The high ionic character and simple structure (rock salt) have made MgO an ideal model system for atomistic simulation of both bulk[13,14] and surface properties.[15]

High-purity metal oxides are most easily prepared by calcining the hydroxides. The hydroxide is usually prepared by hydrolysis of the relevant metal alkoxide using a sol−gel route. Small particle size MgO is generally prepared by this method.[3−5,16−20] Klabunde and co-workers[3−5,19,20] have successfully developed a modified autoclave hypercritical drying procedure to prepare a hydrated form of MgO from $Mg(OCH_3)_2$ that yields high surface area MgO with a particle size of ∼3.5 nm. A variety of techniques have been used to follow the synthesis and study the final form of the material including IR,[18] electron microscopy,[3,20] differential thermal analysis,[3,18] X-ray powder diffraction,[19] and atomic force microscopy.[3] A number of important and interesting features of the route and the resulting MgO have emerged. First, the hydrolysis of the hydroxide produces $Mg(OH)(OCH_3)$ rather than $Mg(OH)_2$.[18−20] Removal of the $-OCH_3$ group is difficult and the calcining

* Author for correspondence. E-mail: M.E.Smith@ukc.ac.uk.

(1) Gleiter, H. *Adv. Mater.* **1992**, *4*, 474.
(2) Henglein, A. *Chem. Rev.* **1989**, *89*, 1061.
(3) Stark, J. V.; Park, D. G.; Lagadic, I.; Klabunde, K. J. *Chem. Mater.* **1996**, *8*, 1904.
(4) Stark, J. V.; Klabunde, K. J. *Chem. Mater.* **1996**, *8*, 1913,
(5) Koper, O.; Lagadic, I.; Klabunde, K. J. *Chem. Mater.* **1997**, *9*, 838.
(6) Liang, S. H. C.; Gay. I. D. *J. Catal.* **1986**, *101*, 293.
(7) Shido, T.; Asakura, K.; Iwasawa, Y. *J. Catal.* **1990**, *122*, 55.
(8) Driscoll, D. J.; Martir, W.; Wang, J. X.; Lunsford, J. H. *J. Chem. Soc., Faraday Trans.* **1990**, *86*, 703.
(9) Lauriente, M. *Insulation* **1959**, *5*, 21.
(10) Tarsa, E. J.; De Graef, M.; Clarke, D. R.; Gossard, A. C.; Speck, J. S. *J. Appl. Phys.* **1993**, *73*, 3276.
(11) Sempolinski, D. R.; Kingery, W. D. *J. Am. Ceram. Soc.* **1980**, *63*, 664.
(12) Cox, P. A.; Henrich, V. E. *The Surface Science of Metal Oxides*; Cambridge University Press: Cambridge, 1994.
(13) Allan, N. L.; Leslie, M.; Mackrodt, W. C. *Ad. Ceram.* **1987**, *23*, 257.
(14) Pisani, C.; Cora, F.; Dovesi, R.; Orlando, R. *J. Electron. Spectrosc. Relat. Phenom.* **1994**, *69*, 1.
(15) De Leeuw, N. H.; Watson, G. W.; Parker, S. C. *J. Phys. Chem.* **1995**, *99*, 17219.
(16) Astier, M.; Bertrand, A.; Bianchi, D.; Chenard, A.; Grades, G. E. E.; Pajonk, G.; Taghavi, M. B.; Teichner, S. J.; Villemin, B. L. *Preparation of Catalysts*; Delmon, B., Jacobs, P. A., Poncelet, G., Eds.; Elsevier: Amsterdam, 1976; p 315.
(17) Teichner, S. J.; Nicalaon, G. A.; Vicarini, M. A.; Gardes, G. E. E. *Adv. Colloid Interface Sci.* **1976**, *5*, 245.
(18) Rywak, A. A.; Burlitch, J. M.; Loehr, T. M. *Chem. Mater.* **1995**, *7*, 2028.
(19) Utamapanya, S.; Klabunde, K. J.; Schlup, J. R. *Chem. Mater.* **1991**, *3*, 175.
(20) Itoh, H.; Utamapanya, S.; Klabunde, K. J.; Schlup, J. R. *Chem. Mater.* **1993**, *5*, 171.

S0897-4756(97)00629-7 CCC: $15.00 © 1998 American Chemical Society
Published on Web 02/07/1998

conditions are crucial in determining the nature of the product. The MgO produced is nanocrystalline, with significant surface coverage by −OH groups and is highly absorptive.[3−5] MgO produced by calcining normally produced $Mg(OH)_2$ is in the form of hexagonal plates (∼150 nm diameter and ∼9 nm thick) with the large exposed face being a (100) plane. In contrast, the autoclave preparation[3] yields 2−6 nm polyhedra with more high index planes exposed at the surface.

Atomic scale structural characterization is increasingly playing a central role in materials synthesis. Solid-state NMR is coming to the fore in materials characterization since its short-range nature means it can identify local coordinations in both crystalline and amorphous materials. ^{17}O is potentially a very useful nucleus that would be widely applicable in materials research. ^{17}O has a wide chemical shift range, making it a sensitive probe of structure, and despite being quadrupolar (nuclear spin $I = {}^5/_2$), it has only a small nuclear electric quadrupole moment (eQ). In ionic materials the closely spherical charge distribution around oxygen produces only small electric field gradients (eq) so that under magic angle spinning (MAS)[21] very high resolution ^{17}O NMR spectra can be produced. The only major drawback of ^{17}O is its low natural abundance (0.037%), so that routine observation requires isotopic enrichment. ^{17}O MAS NMR of enriched ABO_3 and A_2BO_3 compounds produce extremely high resolution spectra from powder samples, with the B cation largely determining the shift, and the number of resonances and their splitting reflecting the symmetry of the structure.[22] Sol−gel materials produced by hydrolysis with ^{17}O-labeled H_2O is a very efficient method of isotopic enrichment. Such an approach has already been applied to a wide range of oxides including ZrO_2,[23] TiO_2,[24] La_2O_3,[25] and HfO_2.[26] This ^{17}O NMR work has shown that the states intermediate to producing the oxides vary widely, for instance, the chemically very similar ZrO_2 and HfO_2 form mixtures of monoclinic and tetragonal local environments in ZrO_2 gels,[23] but only monoclinic environments in HfO_2.[26] The work on TiO_2 determined that the ^{17}O NMR line widths in the intermediate amorphous states result from chemical shift dispersion caused by the range of environments and not the unaveraged second-order quadrupolar interaction. On crystallization there is a sharp decrease in the line width of the ^{17}O MAS NMR spectra as the chemical shift dispersion is greatly reduced. Sol−gel produced oxides are often initially nanocrystalline, which makes detailed analysis by conventional X-ray diffraction (XRD) difficult.

So far there have been few solid-state ^{25}Mg NMR studies since ^{25}Mg has a small gyromagnetic ratio and experiences about an order of magnitude greater second-order quadrupolar broadening than the commonly studied ^{27}Al (for sites with the same eq). If the site symmetry is high, then ^{25}Mg NMR spectra can be relatively easily obtained with reports existing for model compounds,[27] magnesium alloys,[28] and some silicates.[29] The cubic structure of MgO makes it ideal for NMR study by both ^{25}Mg and ^{17}O,[30,31] with a detailed variable-temperature study[31] on bulk polycrystalline MgO showing that from room temperature to 1300 °C the ^{17}O and ^{25}Mg shifts change by 10 and 2 ppm, respectively. This paper uses conventional XRD to give an estimate of crystallite size, in conjunction with ^{17}O and ^{25}Mg NMR to give a detailed picture of the local structure of sol−gel produced nanocrystalline MgO. The development of the atomic scale structure with crystallite size and the influence of residual organic fragments are also examined.

Experimental Section

The preparation of nanocrystalline MgO followed a sol−gel route from magnesium methoxide, $Mg(OCH_3)_2$. A solution of $Mg(OCH_3)_2$ in methanol (Aldrich) was reacted with a slight stoichiometric excess of water in methanol over 24 h. The methanol was then allowed to slowly evaporate off by exposing to the atmosphere. Small samples (1−2 g) of the resulting gel were calcined at various temperatures either in air or under dynamic vacuum (10^{-6} Torr). ^{17}O-enriched samples were prepared in a similar manner except that 10% ^{17}O-enriched H_2O was used and evaporation of methanol was performed under a gentle flow of nitrogen to avoid any exchange reaction with ^{16}O from the atmosphere. Samples were put in a bottle with the normal atmosphere and NMR run within a couple of days. A summary of the heat treatments and the mean crystallite sizes appears in Table 1.

XRD patterns of all the samples were collected on a Phillips PW1050 powder diffractometer using Cu Kα radiation (λ = 0.1544 nm). A range of $2\theta = 10-90°$ was scanned at a rate of 1° min^{-1}. An estimate of the particle size (S) was made from the Debye−Scherrer equation,[32] i.e., $S = K\lambda/(\beta \cos \theta)$, where K is a constant (0.89) and β is the full width at half-height of a diffraction peak at angle θ.

^{17}O NMR spectra were acquired on a Chemagnetics CMX 300 Infinity spectrometer operating at a frequency of 40.18 MHz. A 7.5 mm MAS probe was employed spinning at typically 5 kHz. To ensure that fully relaxed spectra were obtained, 45° pulses of 3.5 μs and recycle times of 10 s for larger particle sizes and 2−5 s for smaller particles (<5 nm) were used with 10^2-10^4 scans necessary depending on the line width. Additionally some static spectra were also collected using a spin−echo with extended phase cycling,[33] with ^1H high-power decoupling. Spectra were shift referenced against H_2O at 0 ppm.

^{13}C NMR spectra were acquired on a Bruker MSL 300 spectrometer operating at 75.465 MHz using a 7 mm MAS probe spinning at typically 4.5 kHz. Cross polarization (CP) was made with rf fields corresponding to 90° pulse widths of 4.6 μs with a contact time of 1 ms and acquired with ^1H decoupling with a field of ∼5 mT, using a recycle time of 4 s

(21) Andrew, E. R. *Int. Rev. Phys. Chem.* **1981**, *1*, 195.
(22) Bastow, T. J.; Dirken, P. J.; Smith, M. E.; Whitfield, H. J. *J. Phys. Chem.* **1996**, *100*, 18539.
(23) Bastow, T. J.; Smith, M. E.; Whitfield, H. J. *J. Mater. Chem.* **1992**, *2*, 989.
(24) Bastow, T. J.; Moodie, A. F.; Smith, M. E.; Whitfield, H. J. *J. Mater. Chem.* **1993**, *3*, 697.
(25) Ali, F.; Smith, M. E.; Steuernagel, S.; Whitfield, H. J. *J. Mater. Chem.* **1996**, *6*, 261.
(26) Bastow, T. J.; Smith, M. E.; Whitfield, H. J. *J. Mater. Chem.* **1996**, *6*, 1951.
(27) Dupree, R.; Smith M. E. *J. Chem. Soc., Chem. Commun.* **1988**, 1483.
(28) Bastow, T. J.; Smith, M. E. *J. Phys.: Condens. Matter* **1995**, *7*, 4929.
(29) MacKenzie, K. J. D.; Meinhold, R. H. *Am. Miner.* **1994**, *79*, 250.
(30) Fedotov, M. A.; Gerasimova, G. F. *React. Kinet. Catal. Lett.* **1983**, *22*, 1977.
(31) Fiske, P. S.; Stebbins, J. F.; Farnan, I. *Phys. Chem. Minerals* **1994**, *20*, 587.
(32) King, H. P.; Alexander, L. E. *X-ray Diffraction Procedures*; Wiley: New York, 1974.
(33) Kunwar, A. C.; Turner, G. L.; Oldfield, E. *J. Magn. Reson.* **1986**, *69*, 124.

Table 1. Summary of Calcination Conditions, Particle Sizes, and ^{17}O and ^{25}Mg NMR Data[a]

	calcination conditions			^{17}O NMR									^{25}Mg NMR	
size (nm)	T (°C)	time (min)	atmos	δ (ppm) ±0.5	Δ (Hz) ±2	% ±2	δ (ppm) ±0.5	Δ (Hz) ±2	% ±2	δ (ppm) ±2	Δ (Hz) ±50	% ±2	δ (ppm) ±0.5	Δ (Hz) ±50
35	700	60	air	47.0	15	100							25.3	450
13.5	625	60	air	47.0	23	68				47	170	32	24.2	610
5	500	30	vacuum	47.0	96	52	42.0	58	3	44	460	45	24.1	965
4.5	300	210	air	47.0	81	47	41.0	76	15	45	920	38	22.3	1200
3	400	60	vacuum	47.0	88	21	42.0	120	24	43	650	55	18.0	1935
2.5	300	60	air	47.0	88	30	41.0	105	20	43	840	50	ND	ND
1.8	300	60	vacuum	47.0	174	5	41.0	235	27	42	1300	68	NM	NM

[a] Size is mean crystallite size determined by XRD, and atmos is the atmosphere used for calcination. The 35 nm sample is sol-gel produced MgO used ^{17}O natural abundance H_2O. δ is the peak position, Δ the full width half-maximum line width, and % is the normalized integrated intensity. Errors quoted are average values for each column. ND, could not be detected; NM, not measured.

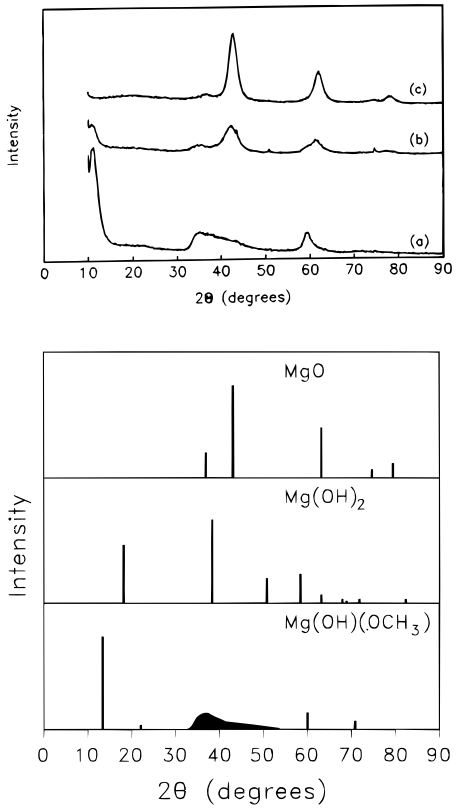

Figure 1. Powder X-ray diffraction patterns of MgO samples calcined in a vacuum for 60 min at (a) 300, (b) 400, and (c) 500 °C. For comparison the standard peak positions of MgO, $Mg(OH)_2$, and $Mg(OH)(OCH_3)$ are shown.

with 500 to 10^4 scans used. The ^{13}C chemical shift was referenced against the CH_2 signal of adamantane at 36.58 ppm.

Additionally some static ^{25}Mg NMR spectra were acquired on the CMX 300 operating at 18.3 MHz using a 5 mm solenoidal coil. Single-pulse excitation using a 2 μs 45° pulse was used with a recycle time of 5 s. 1000−15000 scans were obtained to produce sufficient signal-to-noise depending on the ^{25}Mg line width. ^{25}Mg spectra were referenced against bulk MgO at 26 ppm.[27]

Results

Typical XRD patterns are shown in Figure 1. The patterns from samples heated at 300 °C differ very little from those of unheated samples. It is interesting that this pattern does not correspond to $Mg(OH)_2$ but is characteristic of $Mg(OH)(OCH_3)$, as has been observed by other workers.[18] In this case the estimation of the crystallite size from the Debye−Scherrer equation is very approximate. Samples heated at 400 °C displayed peaks indicative of MgO, although there is still a peak at low angle ($2\theta \sim 10°$), suggesting that the reaction to form MgO is not complete. After calcining at 500 °C the pattern is distinctly that of MgO. In these samples crystallite sizes varied from 1.8 to 100 nm (bulk). A major difference between calcining in air and a vacuum is that in a vacuum the same heating produces smaller crystallite sizes, as can be seen directly by comparing samples heated to 300 °C for 60 min (Table 1).

The ^{17}O MAS NMR spectra show very marked variation with crystallite size. 35 nm MgO gives a single sharp resonance as expected for bulk polycrystalline MgO at 47 ppm. As the particle size decreases, there are marked effects on the ^{17}O center band which broadens and splits (Figure 2). Down to 5 nm the 47 ppm line is the most intense sharp resonance but is clearly accompanied at particle sizes of 5 nm and smaller by a second sharp resolved peak at 41 ppm. To simulate these spectra, Gaussian peaks were chosen on the basis that the MAS line width is dominated by chemical shift dispersion (vide infra), which generally leads to Gaussian line shapes. The 35 nm sample is well simulated by a single Gaussian at the MgO position. For the 13.5 nm sample no single Gaussian can simulate the spectrum, and a second broader underlying peak is required. Although the uniqueness of such a fit cannot be guaranteed given that the line widths of the components differ by more than a factor of 6, using two components is a reasonable choice with as much validity as a continuous distribution or using a non-Gaussian line shape. Then at smaller particle sizes a second narrow Gaussian is required for the second resolved peak (Figure 3). A summary of the parameters required to fit the ^{17}O MAS NMR data is given in Table 1. The 47 ppm line increases in width from 15 Hz in the bulk sample to 90 Hz in the 2.3 nm sample and in the 1.8 nm sample is very poorly defined with a width around 174 Hz. From Figure 2 it is clear that the 47 ppm peak lines up with bulk MgO. Even at a crystallite size of 13.5 nm there is still the need for a broad underlying resonance (Figure 3a). The widths of the second peak at ~41 ppm and the underlying much broader resonance also increase as the crystallite size decreases. The ^{17}O spinning sidebands in the MAS NMR spectra also show a marked variation with particle size (Figure 4). For 13.5 nm particles the main resonance is accompanied by only three sharp, relatively weak sidebands either side extending ±350 ppm. As the particle size decreases, the number of sidebands

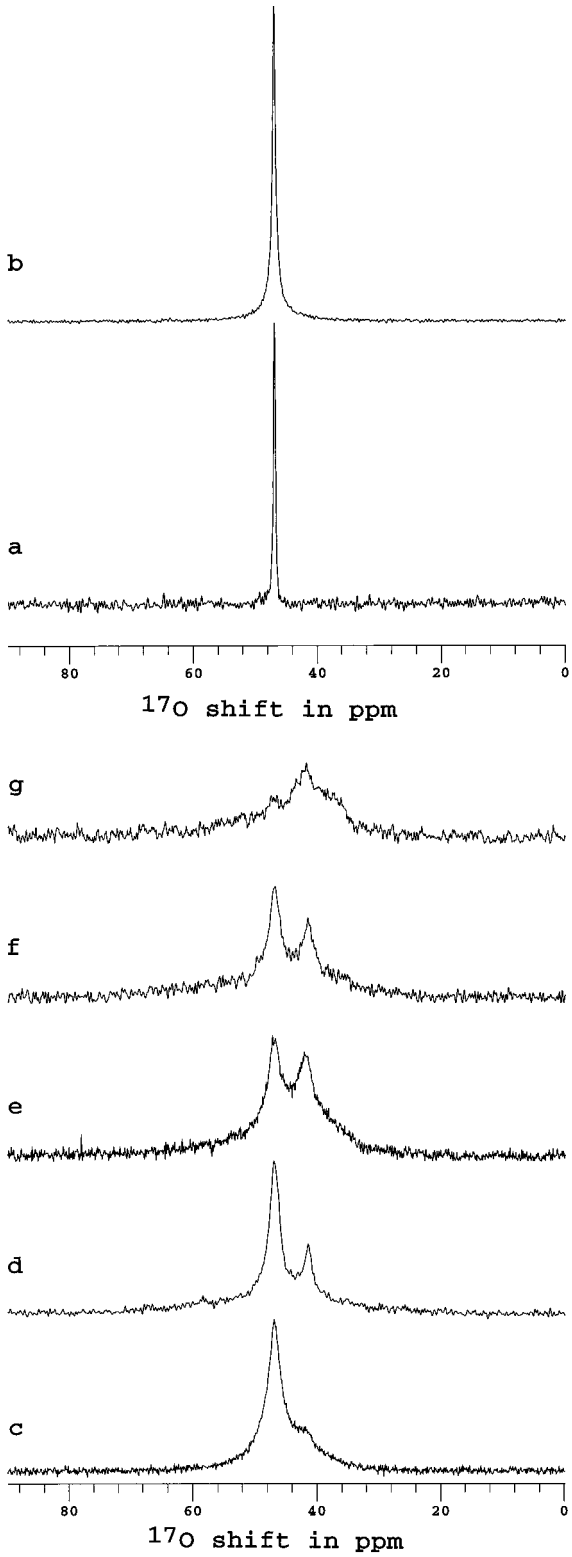

Figure 2. ^{17}O MAS NMR spectra showing the centerbands of MgO with mean crystallite sizes (a) 35, (b) 13.5, (c) 5, (d) 4.5, (e) 3, (f) 2.5, and (g) 1.8 nm.

increase, get broader, and extend at least ±600 ppm. All ^{17}O NMR spectra from these samples were measured a few days after manufacture.

For comparison some static spin−echo ^{17}O NMR spectra were collected. These are much more time-consuming than the MAS spectra and are shown in Figure 5 for the 4.5 nm sample. Comparison is made with and without $^{1}H-^{17}O$ CP. Both spectra show a broad resonance extending over ~45 kHz, which is the resonance from the hydroxyl oxygens. The close association of this resonance with the protons can be seen as this signal cross polarizes very strongly. In the direct experiment there is a second much narrower resonance that shows no CP signal and has none of the structure of MAS spectrum.

^{13}C NMR spectra (Figure 6) show that in those samples that have undergone extensive hydrolysis (which should remove the alkoxide fragments) there is still substantial carbon content. After limited calcination (i.e., at the smaller particle sizes) the main carbon signal comes from CH_3 at ~50 ppm but there is a secondary resonance at ~165 ppm. Care needs to be exercised in comparing absolute signal intensities in Figure 6 and account needs to be taken of the number of scans used and the mass of the sample. Taking these factors into account the peak at 165 ppm is of comparable intensity from the 1.8 and 3 nm samples. The carbon NMR signal intensity decreases with increasing heat treatment, indicating that the total carbon content decreases, and only the peak at 165 ppm remains for the sample with 5 nm crystallites, and even this has become very weak in the 35 nm sample. ^{25}Mg static NMR spectra mirror the trend seen in the ^{17}O MAS NMR, i.e., a resonance that broadens from 35 nm MgO with a line width of 450 Hz to almost 2 kHz in the 3 nm particles and effectively could not be detected in particles smaller than this (Table 1).

Discussion

XRD fixes the approximate mean crystallite size, and NMR provides atomic scale information about structural evolution within these particles as the crystallite size changes. The multinuclear information provided here means that any atomic scale structural picture will have to fit consistently all the NMR data. The ^{17}O information is central as it sees all parts of the structure and the source of the observed MAS line width needs to be determined. In bulk MgO which is cubic the quadrupole coupling constant C_Q ($=e^2qQ/h$) will be zero and very narrow lines are observed. If MgO becomes distorted, by for example disorder, the electric field gradient (efg) will increase. ^{17}O NMR work on oxide gels[24,25] and crystalline mixed metal oxides[22] has determined which factors affect the ^{17}O NMR line width. In crystalline alkali and alkali-earth titanates and zirconates high-resolution spectra are always recorded, and there is very little correlation of the ^{17}O MAS NMR line width (and by implication the efg) with the crystal symmetry. This reflects that although the efg must depend on the site symmetry a much more important factor determining the efg at the oxygen site is the ionicity of the bonding, as first pointed out by Schramm and Oldfield.[34] This can be understood as the efg is dominated by charge close to the nucleus because of the strong inverse cubed distance dependence, hence the charge distribution on the oxygen itself to first order determines the efg with the rest of lattice producing a smaller effect. Hence for highly ionic systems the charge distribution on the oxygen ion will always be closely spherical and the contribution to the efg from even a considerably dis-

(34) Schramm. S.; Oldfield, E. *J. Am. Chem. Soc.* **1984**, *106*, 2502.

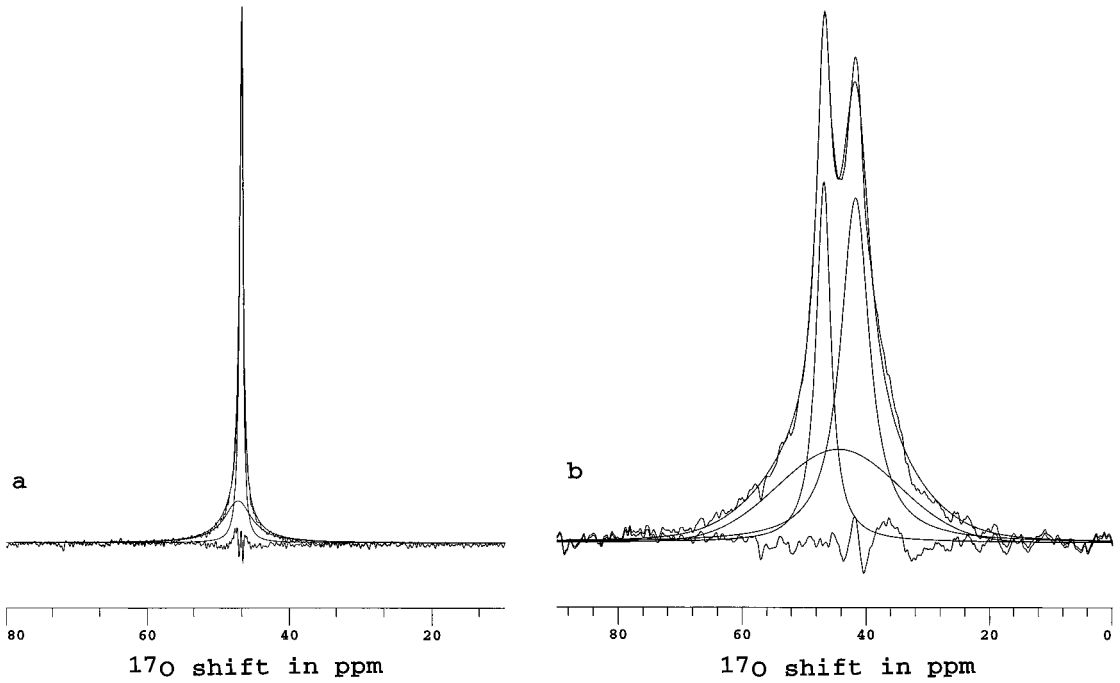

Figure 3. Deconvolution of ^{17}O MAS NMR centerbands for MgO with mean crystallite sizes (a) 13.5 and (b) 3 nm MgO.

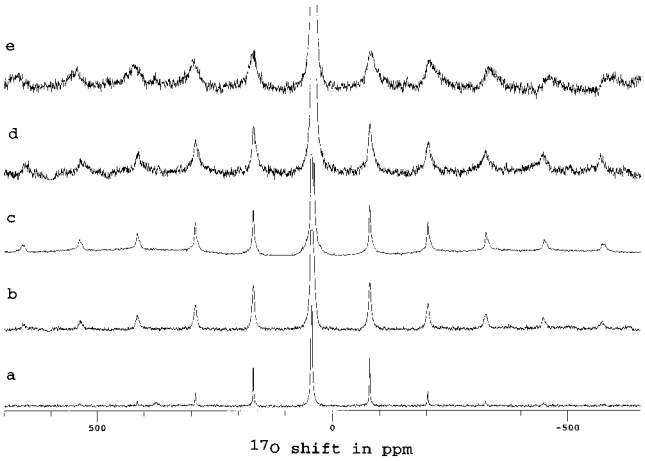

Figure 4. ^{17}O MAS NMR spectra showing the spinning sideband manifolds of MgO with mean crystallite sizes of (a) 13.5, (b) 5, (c) 4.5, (d) 3, and (e)1.8 nm.

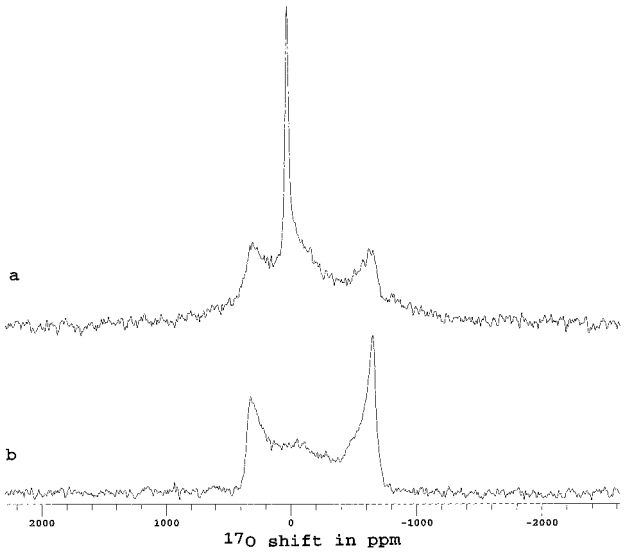

Figure 5. ^{17}O static spin−echo NMR spectra of 4.5 nm MgO (a) direct and (b) cross-polarized.

torted lattice will remain relatively small. This is a crucial point to realize since it explains the low sensitivity of the efg in titanates and zirconates to the structural symmetry. In compounds with more covalent bonds (e.g., silicates, carbonates, hydroxides) the efg rises significantly because of the asymmetry of the local charge distributon close to the oxygen. Hence for the MgO-like (i.e., Mg−O−Mg) part of the structure being highly ionic, the efg will be small even in disordered particles.

To understand the larger line widths from the smaller particle sizes, comparison should be made to the ^{17}O MAS NMR work on TiO_2 and La_2O_3 gels.[24,25] This work showed conclusively that in these ionic oxides that the MAS line widths were almost completely determined by chemical shift dispersion as they scaled directly with the applied magnetic field. Thus in structurally disordered ionic oxides as C_Q will never be very large the MAS line widths can be expected to be determined by the chemical shift dispersion. This range of sites decreases with heat treatment, hence the decrease in the line width. Such observations have been made for TiO_2 and HfO_2 gels.[24,26] The spinning sidebands provide a check on this in that for a spin $^5/_2$ nucleus they will spread out over a range of approximately $3C_Q/5$. It could be argued that there might be some sites where C_Q is so large that the spinning sidebands extend over a broad range and there is insufficient signal-to-noise to observe them here. The increase necessary in C_Q to render the sidebands from Mg−O−Mg fragments unobservable is extremely unlikely for even the most distorted such environment. The sidebands in Figure 4 are attributed to Mg−O−Mg species. As the particle size decreases the extent of the spinning sidebands decreases, but even generously estimating their extent for 3 nm crystallites as ±40 kHz, then $C_Q = 67$ kHz, which would contribute <1 Hz in second-order quadrupolar broadening to the MAS center band, i.e., it makes

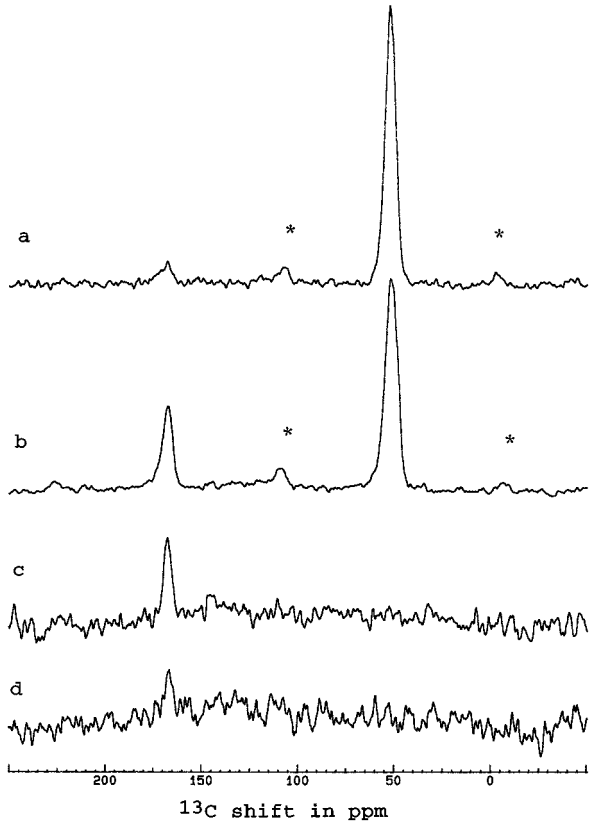

Figure 6. ^{13}C CP MAS NMR spectra of MgO with mean crystallite sizes of (a) 1.8 (480 scans), (b) 3 (10^4), (c) 5 (1960), and (d) 35 nm (1828) (*, spinning sidebands).

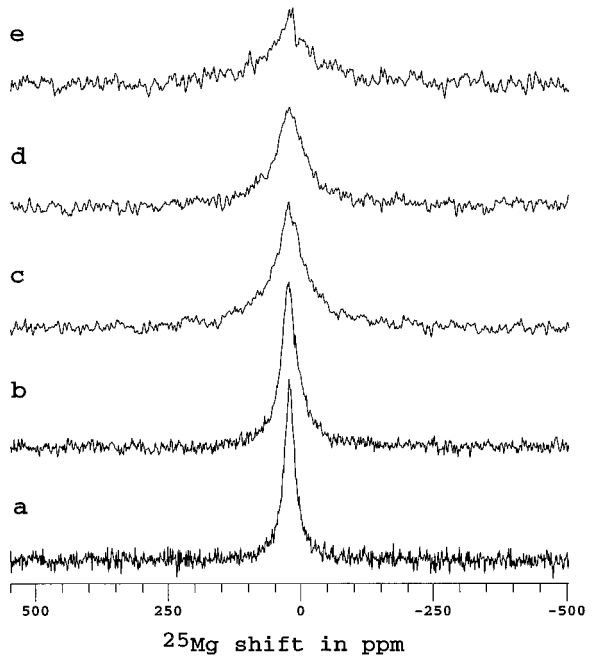

Figure 7. ^{25}Mg static NMR spectra of MgO with mean crystallite sizes of (a) 35, (b) 13.5, (c) 5, (d) 4.5, and (e) 3 nm.

a negligible contribution. Hence the Mg−O−Mg ^{17}O MAS NMR line widths observed here are directly interpretable as a range of environments.

The chemical shift gives a direct indication as to the nature of the environment. The peak at 47 ppm is clearly from an oxygen that is in a "bulk" MgO like environment, simply by comparison of the shift.[35] That is to say, an oxygen that has six magnesium nearest neighbors, and each of these magnesiums will have five other oxygen nearest neighbors. The ^{17}O chemical shift is sensitive and any perturbation in this arrangement will have an effect on the shift, and this is of course the cause of the increased line width *of this peak* in the small particles. It is interesting that even in samples that show broad XRD characteristics of MgO there is ^{17}O NMR evidence of some of the oxygen sites already having the local structure characteristic of MgO with only a moderate spread of sites. Similar observations have been made in many other oxide gels that the local structure takes on characteristic electron densities (that determine the chemical shift) in very early stages of the gel formation.[36]

On the basis of chemical knowledge of the system other structural units present can be postulated. ^{13}C NMR indicates that there is substantial carbon content in the smaller particle sizes in the form of CH_3, and in such materials a $MgOCH_3$ environment would be expected. There is a strong correlation between the intensity of the 41 ppm peak in the ^{17}O NMR spectra and the presence of a ^{13}C CH_3 signal, with both disappearing approximately together. Such a direct assignment of the 41 ppm peak to $MgOCH_3$ is probably mistaken given that C_Q at the oxygen site is strongly linked to the ionicity of the bond.[34] In carbonates where oxygen is effectively bonded only to carbon $C_Q \approx 7$ MHz.[37] In a $MgOCH_3$ linkage even if C_Q is considerably below the value of C_Q in a carbonate as here it is bonded on one side to magnesium, the presence of carbon would still lead to much greater MAS line widths than are measured. Also in the samples that have undergone relatively little calcination there is substantial MgOH bonding which also has a much greater C_Q. As shown in Figure 5, such species can indeed be detected in the small particle size nanocrystalline samples, but only if an echo is used. At MAS of 5 kHz the second-order quadrupolar broadening of $Mg(OH)_2$ will not narrow, and the unnarrowed broad line is then lost in the 30 μs delay used prior to acquisition in the one-pulse sequence used to record Figures 2 and 4. Hence the ^{17}O MAS NMR spectra presented here are filtering out those oxygens attached directly to carbon and hydrogen.

The implication is the three resonances which the ^{17}O MAS NMR spectra have been decomposed into are all "MgO-like" environments, in that they will then correspond to oxygens with six magnesium nearest neighbors. These magnesiums will then have oxygen next nearest neighbors, and then these oxygens can have either nearest-neighbor magnesiums or some other element. The 47 ppm peak is most likely only magnesiums at the third-nearest-neighbor level. The circumstantial evidence is that 41 ppm looks like "bulk" MgO except that one of these third nearest neighbors is probably a carbon (or proton). So in a one-dimensional picture in the case of the 47 ppm resonance if O* is the contributing oxygen, this would correspond to (Mg-OMgO*MgOMg), whereas that at 41 ppm is (MgO-MgO*$MgOCH_3$ (or H)). The relatively narrow line

(35) Turner, G. L.; Chung, S. E.; Oldfield, E. *J. Magn. Reson.* **1985**, *64*, 316.
(36) Bastow, T. J.; Murgaski, L.; Smith, M. E.; Whitfield, H. J. *Mater. Lett.* **1995**, *4*, 313.
(37) Smith, M. E.; Steuernagel, S.; Whitfield, H. J. *Solid State NMR* **1995**, *4*, 313.

width (compared to the underlying line) is an indication that the primary factors determining the line width are MgO-like, and there is only a small perturbation affecting the isotropic shift. That this influence can be caused by a third nearest neighbor underlines the exquisitely sensitive nature of the ^{17}O chemical shift which is being postulated here as effectively probing medium-range order. Then there is the much broader underlying peak that persists up to quite large particle sizes, well after the CH_3 peak is lost from the ^{13}C NMR spectrum. The shift at around 45 ppm is indicative of an MgO-like environment, but the much larger width indicates a greater range of this environment. In particles that are made up of nanocrystalline domains the surface of each nanocrystallite makes up a sizable volume fraction of the sample. At surfaces there is some relaxation of the structure which leads to a wider range of environments, hence producing a broader resonance. The number of layers that can be regarded as surface is not clear, but if two layers are "surface" for a cubic 3 nm particle, 46% of the oxygen is in such a "surface". Again based on circumstantial evidence of the underlying peak increasing in intensity as the crystallite size decreases (and hence the volume associated with the surface increases), this underlying resonance belongs to surface MgO.

In sol−gel produced MgO in the nanocrystalline particles ^{13}C NMR shows that carbon fragments persist as CH_3, even though extensive hydrolysis has occurred. On calcination CH_3 is removed, probably as methanol by reaction with residual hydroxyls present. The other carbon corresponding to the 165 ppm peak is probably carbonate,[38] which is formed by surface reaction with CO_2, as the peak is larger in smaller size particles. In the 1.8 nm sample it must be remembered that far fewer scans were used than for the 3 nm sample and also that the presence of much larger amounts of CH_3 might make the surface much less reactive with respect to CO_2. (Note that bulk MgO taken from the bottle without any calcination often shows detectable surface carbonate formation.) Overall the total carbon signal decreases with increasing heat treatment and effectively all carbon can be removed at sufficiently high temperature.

(38) Papenguth, H. W.; Kirkpatrick, R. J.; Montez. B.; Sandberg, P. A. *Am. Mineral.* **1989**, *74*, 1152.

NMR produces a detailed picture of the atomic scale structural development of MgO. Initially Mg(OH)-(OCH_3) forms and in the ^{17}O MAS NMR spectra there is some broad ill-defined intensity that corresponds to MgO-like environments, but at this point must be very highly disordered. In samples where broad MgO reflections appear, corresponding to a crystallite size of ∼3 nm, with significant carbon content, in addition to the MgOH and $MgOCH_3$ environments there are now some genuine MgO-like species. ^{17}O MAS NMR reveals three MgO-like environments that can be attributed to that which is essentially already bulk MgO-like (47 ppm), but with some site variation causing increased line width compared to bulk polycrystalline MgO. There is a second site (41 ppm) that is almost like bulk MgO except that it is perturbed probably by the presence of H or CH_3 at the third-nearest-neighbor level, and a broader line that is associated here with surface layers. As calcination proceeds the particle size increases and carbon (and hydroxyl) is removed, and there is a decrease in the intensity of the 41 ppm ^{17}O resonance as well as of the broader underlying resonance. Eventually all the ^{17}O intensity becomes like bulk MgO at 47 ppm. Such high structural sensitivity should make ^{17}O NMR extremely useful in characterizing defect sites in doped MgO.

Conclusion

Nanocrystalline MgO can be effectively manufactured by a sol−gel process with the crystallite size controlled by calcination. Multinuclear magnetic resonance is an extremely sensitive probe of local structure. ^{13}C NMR shows the presence of CH_3 fragments even after significant calcination. ^{25}Mg NMR can be readily recorded, except in the smallest particles where significant chemical shift dispersion broadening occurs. Three MgO-like environments are observed in the ^{17}O MAS NMR spectra, with two related to bulklike environments and the third due to the surface layers.

Acknowledgment. Funding of work on nanocrystalline oxides by the EPSRC is gratefully acknowledged (GR/K74876), and M.E.S. thanks the University of Kent for supporting solid-state NMR and NERC.

CM970629+